NACA RM L51K16a

NACA

RESEARCH MEMORANDUM

AERODYNAMIC CHARACTERISTICS AT SUPERSONIC SPEEDS OF A SERIES OF WING-BODY COMBINATIONS HAVING CAMBERED WINGS WITH AN ASPECT RATIO OF 3.5 AND A TAPER RATIO OF 0.2

EFFECTS OF SWEEP ANGLE AND THICKNESS RATIO ON THE AERODYNAMIC CHARACTERISTICS IN PITCH AT M = 1.60

By Ross B. Robinson and Cornelius Driver

Langley Aeronautical Laboratory
Langley Field, Va.

NATIONAL ADVISORY COMMITTEE FOR AERONAUTICS

WASHINGTON

January 10, 1952
Declassified May 16, 1958

NATIONAL ADVISORY COMMITTEE FOR AERONAUTICS

RESEARCH MEMORANDUM

AERODYNAMIC CHARACTERISTICS AT SUPERSONIC SPEEDS OF A SERIES OF WING-BODY COMBINATIONS HAVING CAMBERED WINGS WITH AN ASPECT RATIO OF 3.5 AND A TAPER RATIO OF 0.2

EFFECTS OF SWEEP ANGLE AND THICKNESS RATIO ON THE AERODYNAMIC CHARACTERISTICS IN PITCH AT M = 1.60

By Ross B. Robinson and Cornelius Driver

SUMMARY

An investigation has been conducted in the Langley 4- by 4-foot supersonic pressure tunnel at a Mach number of 1.60 and a Reynolds number of 2.7×10^6, based on the wing mean aerodynamic chord, to determine the effects of sweep and thickness on the longitudinal characteristics of a series of wing-body combinations having cambered wings with an aspect ratio of 3.5 and taper ratio of 0.2. The wings, tested on a slender body of revolution, had quarter-chord sweep angles of 10.8°, 35°, and 47° for a thickness ratio of 4 percent, and thickness ratios of 4, 6, and 9 percent for a quarter-chord sweep angle of 47°. In addition, a wing of 47° sweep was tested with thickened root sections. For this wing, the thickness ratios tapered linearly from 12 percent at the root to 6 percent at the 40-percent semispan station and were constant at 6 percent further outboard. The effects of the addition of a horizontal canard surface to the 6-percent-thick, 47° swept wing configuration were also investigated.

The results of this investigation show the effects of sweep, thickness, and the horizontal canard surface on the lift, drag, and pitching-moment coefficients and lift-drag ratios. In addition, lift-curve slopes, aerodynamic-center locations, maximum lift-drag ratios, lift coefficients for maximum lift-drag ratio, and drag-rise factor are presented.

INTRODUCTION

A research program has been in progress at the Langley Aeronautical Laboratory to determine at subsonic, transonic, and supersonic speeds the effects of thickness and sweep on the aerodynamic characteristics of a series of wing-body combinations with cambered wings having a taper ratio of 0.2 and an aspect ratio of 3.5. The effects of thickness on the longitudinal characteristics of a 47° sweptback-wing - body combination at subsonic and transonic speeds are presented in reference 1. The effects of sweep and thickness on the lateral characteristics of the wing series at a Mach number of 1.60 are presented in reference 2. The results of tests at a Mach number of 1.60 of several nacelle configurations on the 6-percent-thick 47° swept wing configuration are given in reference 3.

The present paper gives the results of tests to determine the effects of sweep and thickness on the longitudinal characteristics of this series of wings at a Mach number of 1.60 and a Reynolds number of 2.7×10^6 based on the wing mean aerodynamic chord. The wings had quarter-chord sweep angles of 10.8°, 35°, and 47° for a thickness ratio of 4 percent and thickness ratios of 4, 6, and 9 percent for a sweep angle of 47°. A thickened-root wing of 47° sweep, having a thickness ratio of 12 percent at the root, tapering to 6 percent at the 40-percent semispan station, and remaining constant at 6 percent further outboard was also investigated. The effects of the addition of a horizontal canard surface to the 6-percent-thick 47° swept wing configuration were investigated. These results are presented without analysis to expedite issuance.

SYMBOLS

C_L	lift coefficient of wing-body combination (Lift/qS)
C_D	drag coefficient of wing-body combination (Drag/qS)
C_m	pitching-moment coefficient of wing-body combination about 0.25 mean aerodynamic chord (Pitching moment/qS$\bar{c}$)
C_{L_f}	lift coefficient of body (Lift/qA)
C_{D_f}	drag coefficient of body (Drag/qA)
C_{m_f}	pitching-moment coefficient of body (Pitching moment/qAl)
A	maximum cross-sectional area of body, 0.0276 square foot
S	wing area, 1.143 square feet

$\bar{c}$	wing mean aerodynamic chord, feet
l	body length, feet
q	free-stream dynamic pressure, pounds per square foot
M	Mach number
t/c	streamwise wing thickness ratio
L/D	lift-drag ratio
C_{L_α}	lift-curve slope
$\Delta C_D/C_L{}^2$	drag rise factor
α	angle of attack of body center line, degrees
Λ	sweep angle of wing quarter chord line, degrees

Subscripts:

max	maximum
min	minimum

APPARATUS AND MODELS

Tunnel

The tests were conducted in the Langley 4- by 4-foot supersonic pressure tunnel. This tunnel, described in reference 4, was originally powered by a 6000-horsepower drive motor. Recent modifications to the tunnel have increased the horsepower rating to 45,000. The additional power has resulted in an increase in the maximum stagnation pressure from about 0.3 atmosphere to about 2 atmospheres. The design Mach number range of 1.2 to 2.2 remains unchanged. In addition, the original mild-steel flexible nozzle walls (reference 4) have been replaced by machined-stainless-steel walls. At a Mach number of 1.60 the test section has a width of 4.5 feet, a height of 4.4 feet, and a region of uniform flow which is 7 feet long at the flexible walls. An external air-drying system supplies air of a sufficiently low dew point to prevent moisture condensation in the test section.

Models

The models used in these tests were composed of an ogive-cylinder body and various midwing configurations with a ratio of body diameter to wing span of about 0.094. The models were designed to accommodate solid steel wings with integral cylindrical sections simulating corresponding sections of the body. This design permitted interchange of wings with minimum delay. The wings were positioned so that the quarter-chord point of the mean aerodynamic chord was always at the same body station. The wing airfoil sections had an NACA 65A series thickness distribution and mean-line ordinates 1/3 of NACA 230 plus (a = 1) for $C_L = 0.1$. The airfoil coordinates are given in table I. Details of the models are shown in figure 1.

The models were sting-supported and had a six-component internal strain-gage balance in the body. The model and sting are shown in figure 2. Figure 3 is a photograph of the model in the tunnel. The models, balance, and indicating system were furnished by a U. S. Air Force contractor.

TESTS

Test Conditions

The conditions for the tests of the wing-body configurations were:

Mach number	1.60
Reynolds number, based on wing mean aerodynamic chord	2.7×10^6
Stagnation dew point, degrees Fahrenheit	< 25
Stagnation pressure, atmospheres	1
Stagnation temperature, degrees Fahrenheit	110

In order to establish an indication of the type of boundary layer existing over the basic body to provide a means of assessing the wing drag increments, the body alone was tested through a pressure range of about 4 pounds per square inch to 15 pounds per square inch corresponding to a Reynolds number range of 2.5 to 9×10^6 (based on body length). All the other test conditions remained unchanged.

A limited calibration prior to these tests has shown that the flow in the test section is reasonably uniform. The magnitudes of the variations in the flow parameters are summarized in the following table:

Mach number	± 0.01
Flow angle in horizontal plane, degrees	± 0.1
Flow angle in vertical plane, degrees	± 0.1

Test Procedure

Tests of the wing-body configurations were made through an angle-of-attack range from -2° to 13° and tests of the body of revolution from -2° to 14°.

Corrections and Accuracy

The angle of attack of the model was corrected for deflection of the balance due to lift and pitching moment. Angle corrections were obtained from bench calibration of the balance for various lift loads and pitching moments. The validity of these corrections was verified by comparison with angle corrections measured optically during tests of the 9-percent-thick 47° swept wing. The estimated accuracy of the wing angle of attack was $\pm 0.1^\circ$. During these tests the model was yawed about -0.2° due to misalinement. No corrections were applied for this yaw angle or for the flow variations in the test section.

The estimated errors in the force data were as follows:

C_L	± 0.005
C_D	± 0.001
C_m	± 0.001

The base pressure was measured and the drag data were corrected to correspond to a base pressure equal to free-stream static pressure.

RESULTS

The results are presented without analysis in order to expedite issuance. In order to simulate more closely full-scale characteristics and eliminate drag increments caused by transition of the body boundary layer from laminar to turbulent flow caused by the addition of the wing, the body alone was tested through a Reynolds number range of 2.5×10^6 to 9×10^6 (based on the body length). The drag coefficient obtained during these tests is presented in figure 4 as a function of Reynolds number. On the basis of these data (fig. 4), it was concluded that the boundary-layer flow over the body alone was primarily turbulent above a Reynolds number of 7×10^6 (stagnation pressure of 12 lb/sq in.) and all further tests of the body and the wing-body combinations were therefore conducted at a stagnation pressure of about 15 pounds per square inch.

The experimental aerodynamic characteristics in pitch of the body alone and the theoretical values calculated by the method of reference 5 are presented in figure 5. The aerodynamic characteristics in pitch of the 4-percent-thick wings in the sweep series are shown in figures 6(a) to 6(c), and of the 47° swept wings in the thickness series in figures 6(c) to 6(f). The effect of the addition of a horizontal canard surface to the 6-percent-thick 47° swept wing configuration are shown in figure 7. Schlieren pictures of the wing-body canard configuration are shown in figure 8. The lift-drag ratios as a function of lift coefficient for the wing series are summarized in figure 9: the effects of the addition of the canards in figure 9(a), the effects of thickness in figure 9(b), and the effects of sweep in figure 9(c). The variation of the minimum drag coefficient with the square of the thickness ratio is presented in figure 10. Included for reference purposes on this figure are the experimental body drag coefficient and the theoretical pressure drag coefficient of the body (reference 6). The increment between the body-alone drag coefficient and the extrapolated wing-body drag coefficient for zero wing thickness is an indication of the wing skin friction drag.

A summary of the variation of the longitudinal characteristics with thickness ratio and sweep angle is presented in figure 11 and table II. In general, for this series of wings, the effects of thickness are of the same magnitude as the effects of sweep on the longitudinal characteristics of the wings.

Langley Aeronautical Laboratory
National Advisory Committee for Aeronautics
Langley Field, Va.

REFERENCES

1. Bielat, Ralph P., Harrison, Daniel E., and Coppolino, Domenic A.: An Investigation at Transonic Speeds of the Effects of Thickness Ratio and of Thickened Root Sections on the Aerodynamic Characteristics of Wings with 47° Sweepback, Aspect Ratio 3.5, and Taper Ratio 0.2 in the Slotted Test Section of the Langley 8-Foot High-Speed Tunnel. NACA RM L51I04a, 1951.

2. Spearman, M. Leroy, and Hilton, John H., Jr.: Aerodynamic Characteristics at Supersonic Speeds of a Series of Wing-Body Combinations Having Cambered Wings with an Aspect Ratio of 3.5 and a Taper Ratio of 0.2. Effects of Sweep Angle and Thickness Ratio on the Static Lateral Stability Characteristics at M = 1.60. NACA RM L51K15a, 1951.

3. Hasel, Lowell E., and Sevier, John R., Jr.: Aerodynamic Characteristics at Supersonic Speeds of a Series of Wing-Body Combinations Having Cambered Wings with an Aspect Ratio of 3.5 and a Taper Ratio of 0.2. Effect at M = 1.60 of Nacelle Shape and Position on the Aerodynamic Characteristics in Pitch of Two Wing-Body Combinations with 47° Sweptback Wings. NACA RM L51K14a, 1951.

4. Cooper, Morton, Smith, Norman, F., and Kainer, Julian H.: A Pressure-Distribution Investigation of a Supersonic Aircraft Fuselage and Calibration of the Mach Number 1.59 Nozzle of the Langley 4- by 4-Foot Supersonic Tunnel. NACA RM L9E27a, 1949.

5. Allen, H. Julian: Estimation of the Forces and Moments Acting on Inclined Bodies of Revolution of High Fineness Ratio. NACA RM A9I26, 1949.

6. Lighthill, M. J.: Supersonic Flow past Bodies of Revolution. R. & M. No. 2003, British A.R.C., 1945.

7. Harmon, Sidney M., and Jeffreys, Isabella: Theoretical Lift and Damping in Roll of Thin Wings with Arbitrary Sweep and Taper at Supersonic Speeds. Supersonic Leading and Trailing Edges. NACA TN 2114, 1950.

TABLE I

AIRFOIL COORDINATES FOR THE VARIOUS WINGS

[Thickness distribution: NACA 65A series. Mean-line ordinates: 1/3 of NACA 230 plus (a = 1) for $C_L = 0.1$]

(a) $\frac{t}{c} = 0.04$.

x/c	y/c	
	Upper surface	Lower surface
0	0	0
.5	.411	.245
.75	.499	.271
1.25	.665	.289
2.5	.962	.324
5.0	1.435	.367
7.5	1.776	.429
10	2.039	.472
15	2.423	.577
20	2.642	.682
25	2.800	.787
30	2.887	.892
35	2.983	.997
40	2.992	1.006
45	2.940	1.041
50	2.852	1.006
55	2.712	.945
60	2.511	.857
65	2.265	.761
70	1.986	.674
75	1.680	.577
80	1.356	.481
85	1.041	.385
90	.726	.289
95	.402	.201
100	.105	.105
Tangent point	80.00	60.00
L.E. radius = 0.0016c		

(b) $\frac{t}{c} = 0.06$.

x/c	y/c	
	Upper surface	Lower surface
0	0.061	0
.5	.577	.376
.75	.717	.446
1.25	.919	.534
2.5	1.304	.621
5.0	1.872	.761
7.5	2.318	.857
10	2.668	.980
15	3.150	1.269
20	3.482	1.496
25	3.701	1.697
30	3.858	1.846
35	3.946	1.960
40	3.981	2.021
45	3.937	2.030
50	3.823	1.977
55	3.613	1.872
60	3.342	1.697
65	3.018	1.487
70	2.651	1.277
75	2.231	1.059
80	1.785	.849
85	1.339	.639
90	.892	.420
95	.446	.210
100	0	0
L.E. radius = 0.0024c		

(c) $\frac{t}{c} = 0.09$.

x/c	y/c	
	Upper surface	Lower surface
0	0.156	0
.5	.846	.574
.75	1.021	.680
1.25	1.283	.846
2.5	1.789	1.069
5.0	2.537	1.400
7.5	3.111	1.662
10	3.577	1.896
15	4.244	2.352
20	4.705	2.751
25	5.045	3.052
30	5.288	3.276
35	5.415	3.441
40	5.473	3.529
45	5.424	3.519
50	5.249	3.422
55	4.967	3.208
60	4.579	2.916
65	4.102	2.566
70	3.568	2.197
75	2.975	1.837
80	2.382	1.468
85	1.789	1.098
90	1.186	.739
95	.593	.369
100	0	0
L.E. radius = 0.0056c		

(d) Thickened root.

x/c	y/c at root station	
	Upper surface	Lower surface
0	0.301	0
.5	1.120	.754
.75	1.335	.904
1.25	1.658	1.141
2.5	2.261	1.507
5.0	3.208	2.024
7.5	3.919	2.433
10	4.500	2.799
15	5.362	3.445
20	5.965	3.984
25	6.395	4.414
30	6.718	4.716
35	6.912	4.910
40	6.977	5.017
45	6.912	4.996
50	6.675	4.823
55	6.288	4.522
60	5.771	4.113
65	5.168	3.618
70	4.457	3.101
75	3.725	2.584
80	2.929	2.067
85	2.239	1.550
90	1.486	1.034
95	.732	.517
100	0	0
L.E. radius = 0.0099c		

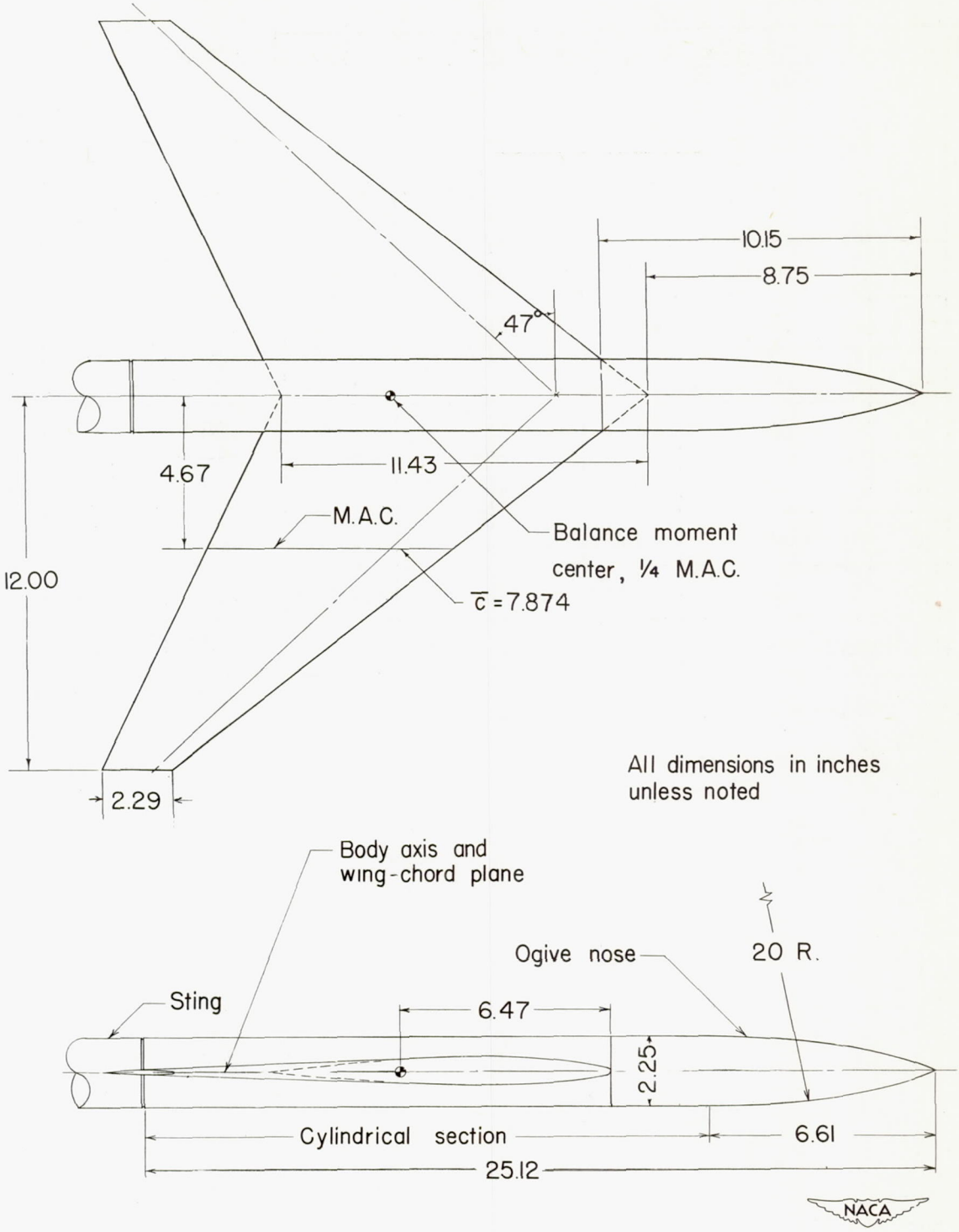
NACA

TABLE II

SUMMARY OF THE LONGITUDINAL CHARACTERISTICS

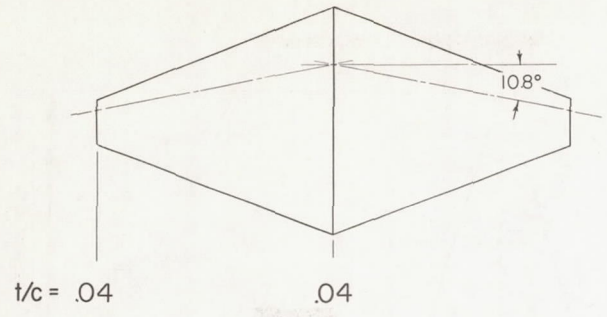
Λ (deg)	t/c	C_{L_α}	$C_{M_{C_L}}$	$C_{D_{min}}$	$\Delta C_D/C_L{}^2$	$(L/D)_{max}$	C_L for $(L/D)_{max}$	a.c.
10.8	0.04	0.0525	-0.188	0.021	0.308	6.41	0.25	0.438
35	.04	.0535	-.230	.019	.308	6.97	.23	.480
47	.04	.053	-.258	.016	.288	7.65	.225	.508
47	.06	.052	-.259	.021	.31	6.28	.25	.509
[1]47	.06	.052	-.200	.022	.299	6.33	.27	.450
47	.09	.048	-.233	.0303	.33	5.10	.29	.483
47	.12, .06, .06	.050	-.260	.026	.308	5.71	.28	.510
Body alone		.0024	.770	.006	-----	----	-----	-.520

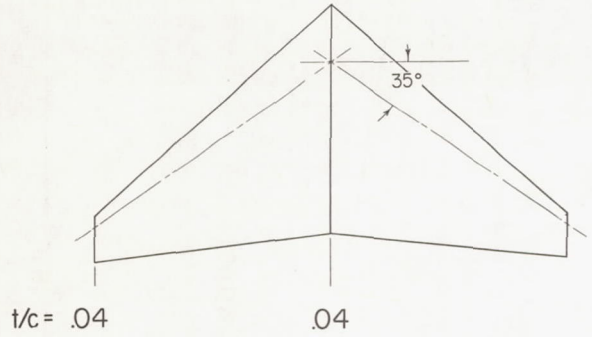
[1]Wing-body canard configuration.



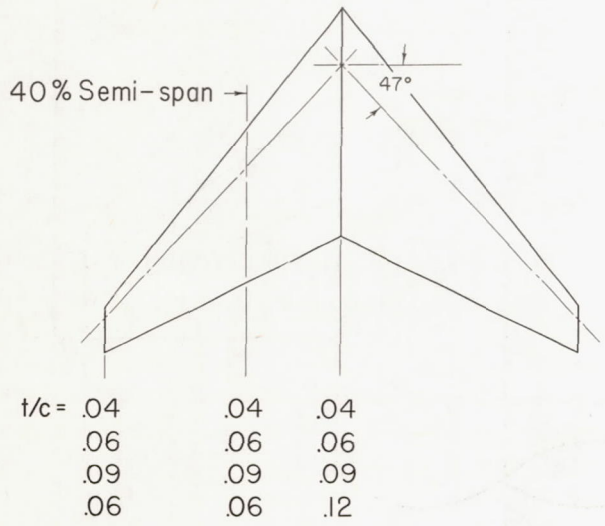
(a) Wing-body arrangement.

Figure 1.- Details of model configurations.





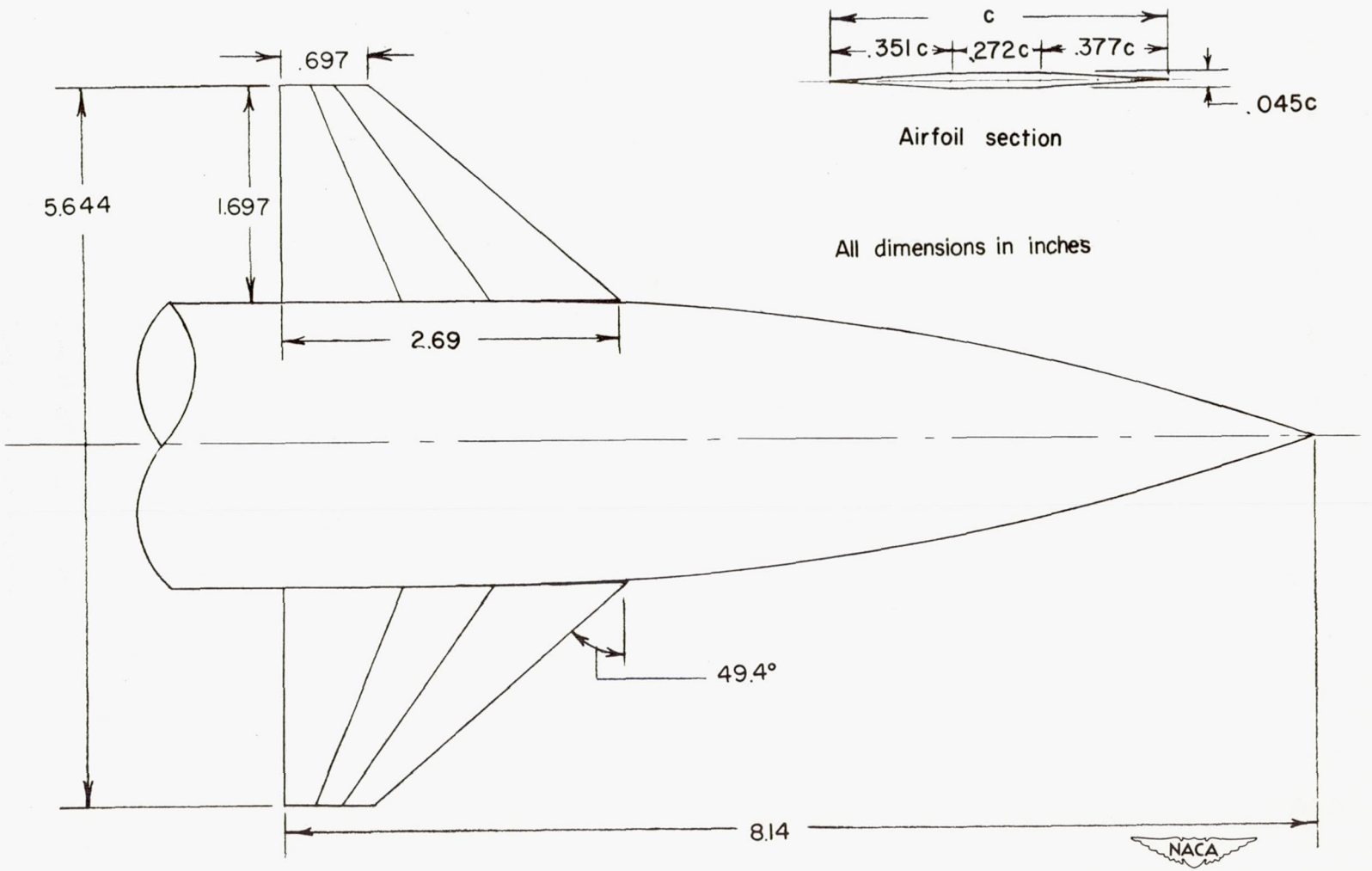
Aspect Ratio	3.5
Taper Ratio	0.2
Span, inches	24
Area, sq. feet	1.143



NACA

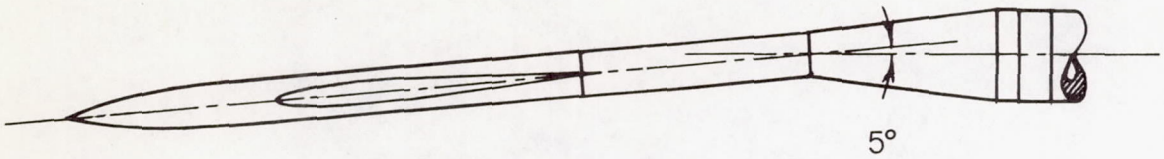
(b) Details of wings.

Figure 1.- Continued.

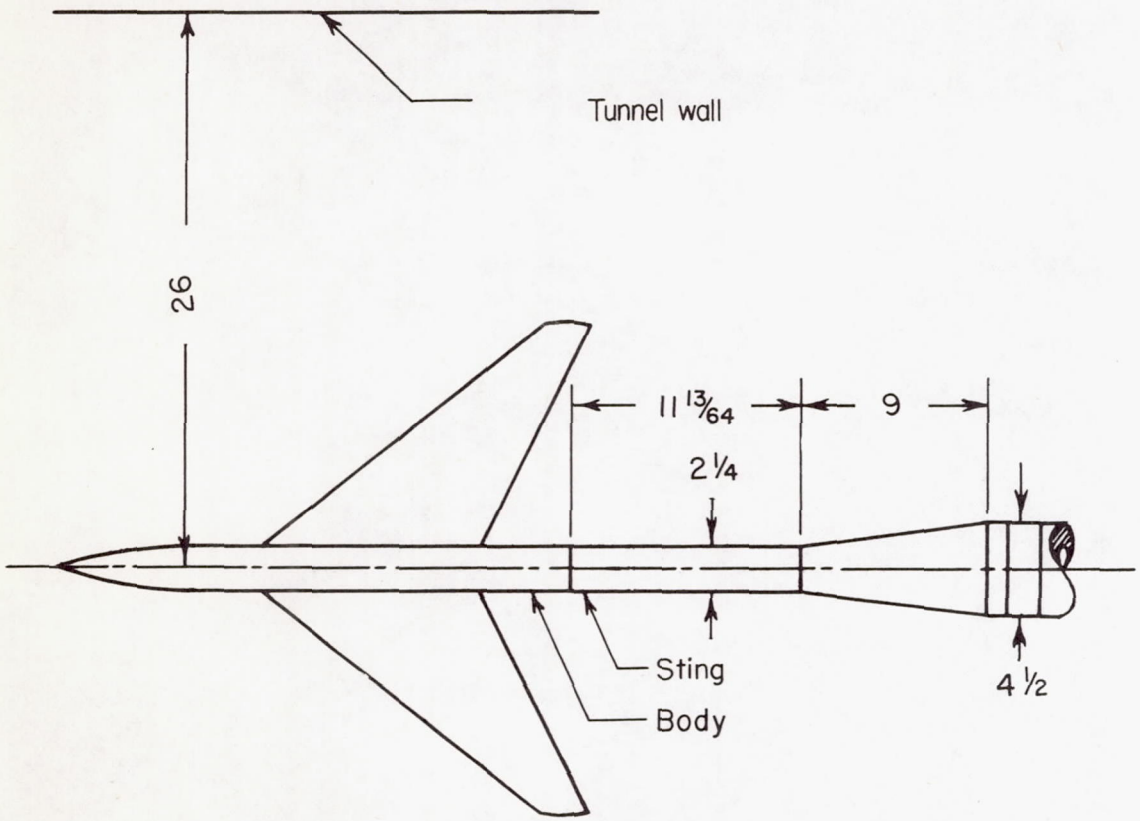


(c) Horizontal canard surface.

Figure 1.- Concluded.



Top view of installation



Side view of installation

Figure 2.- Details of model sting support. All dimensions are in inches unless noted.



Figure 3.- Model mounted for pitch test.

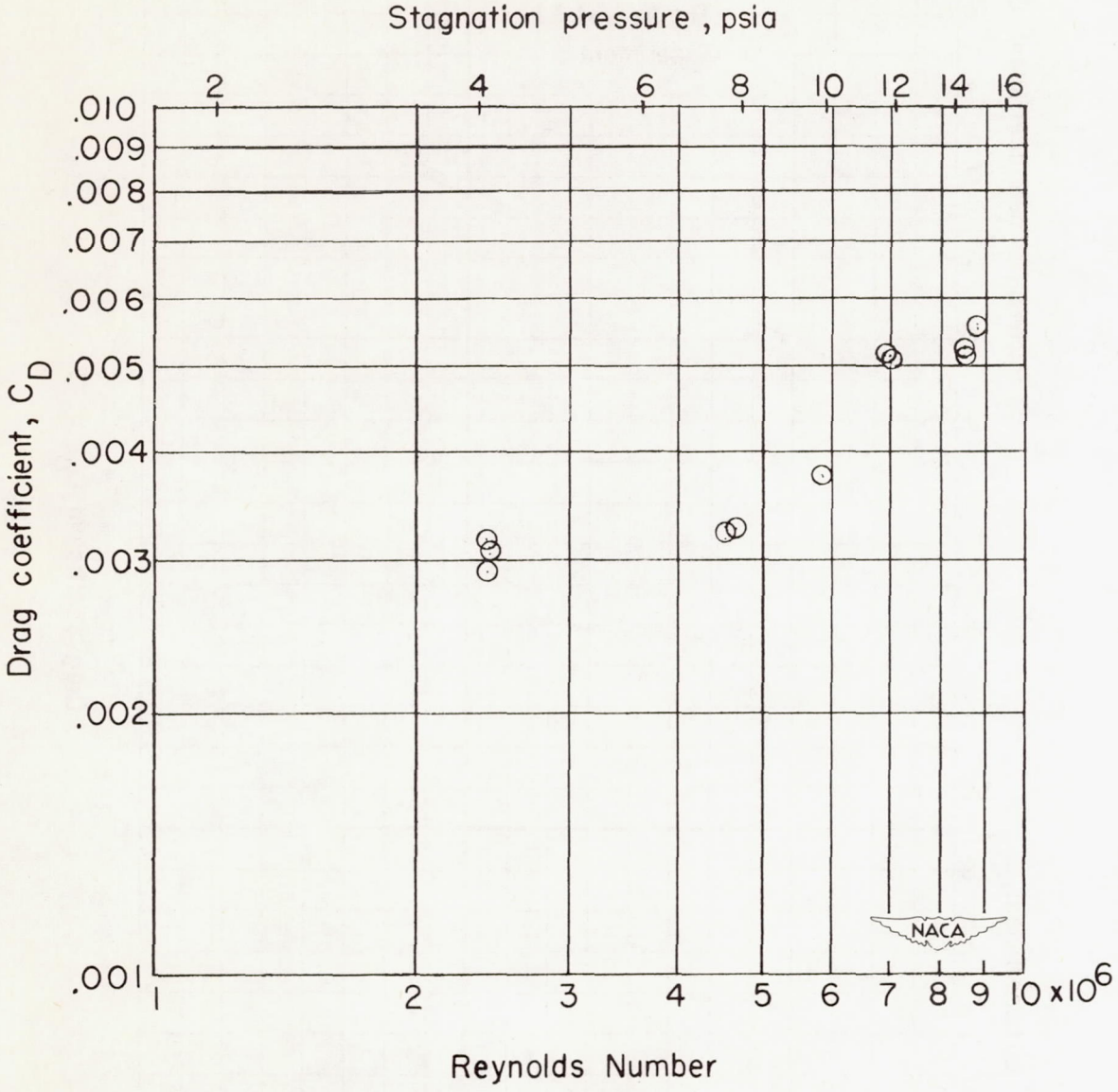


Figure 4.- Variation of body drag coefficient with Reynolds number based on body length.

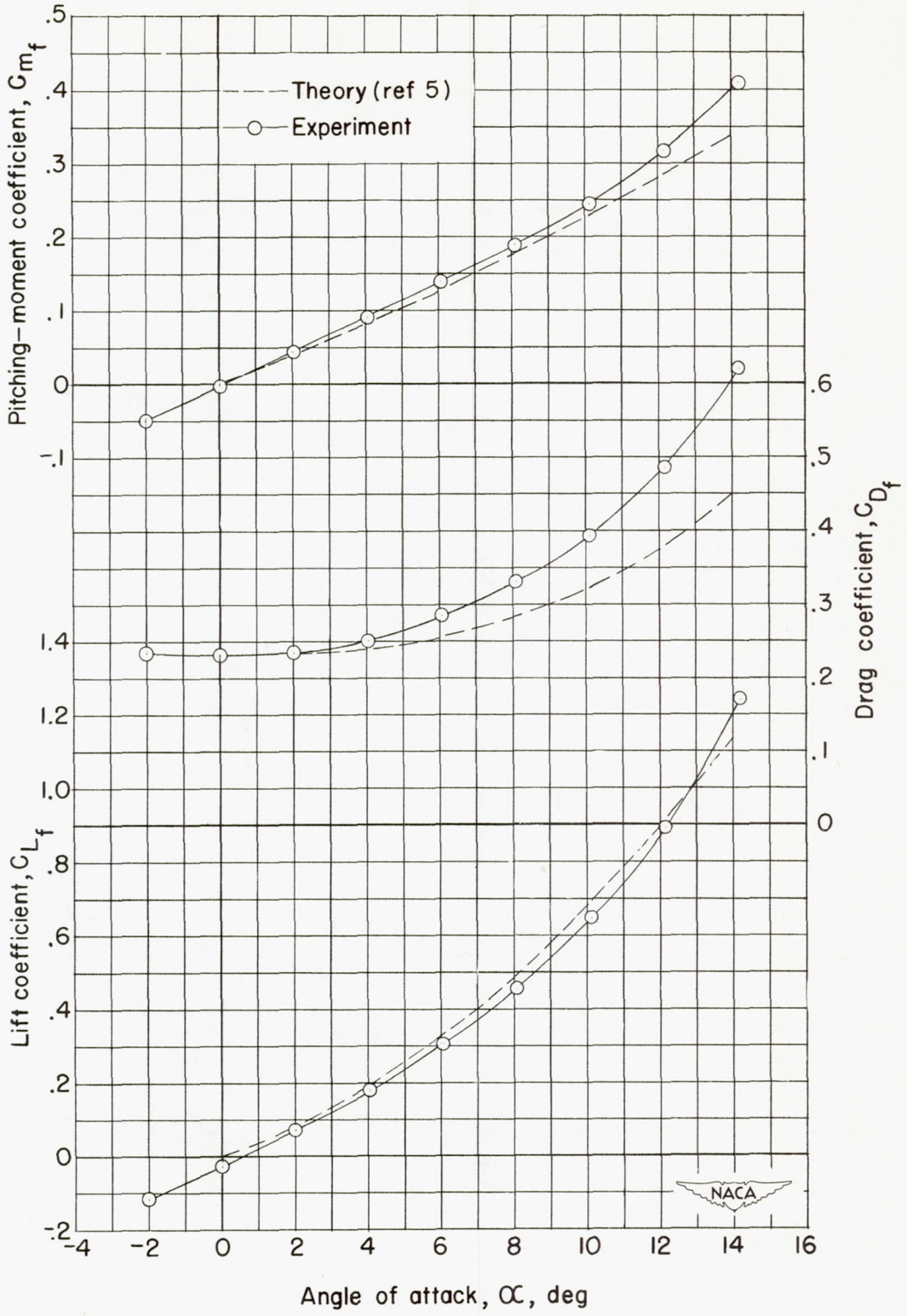
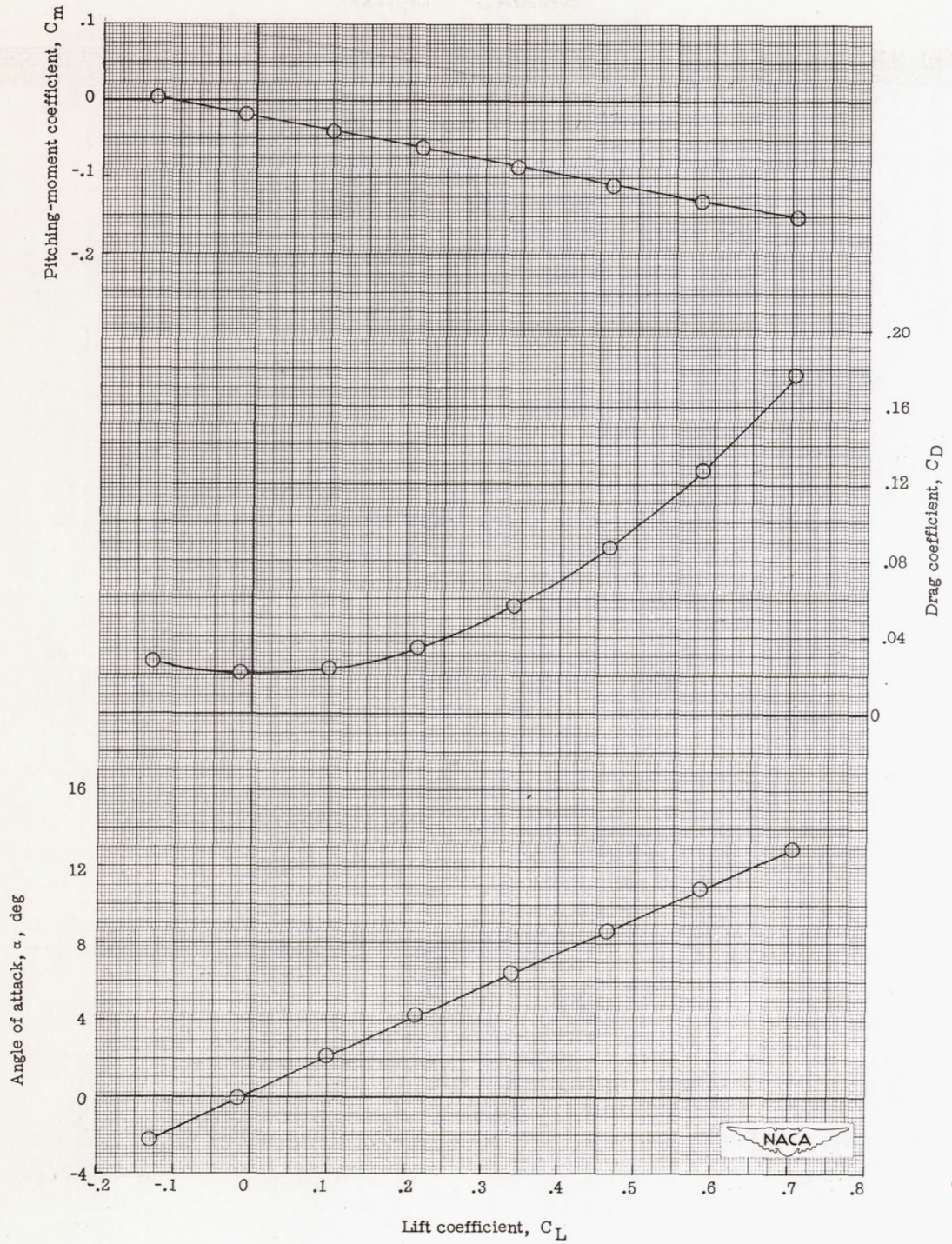
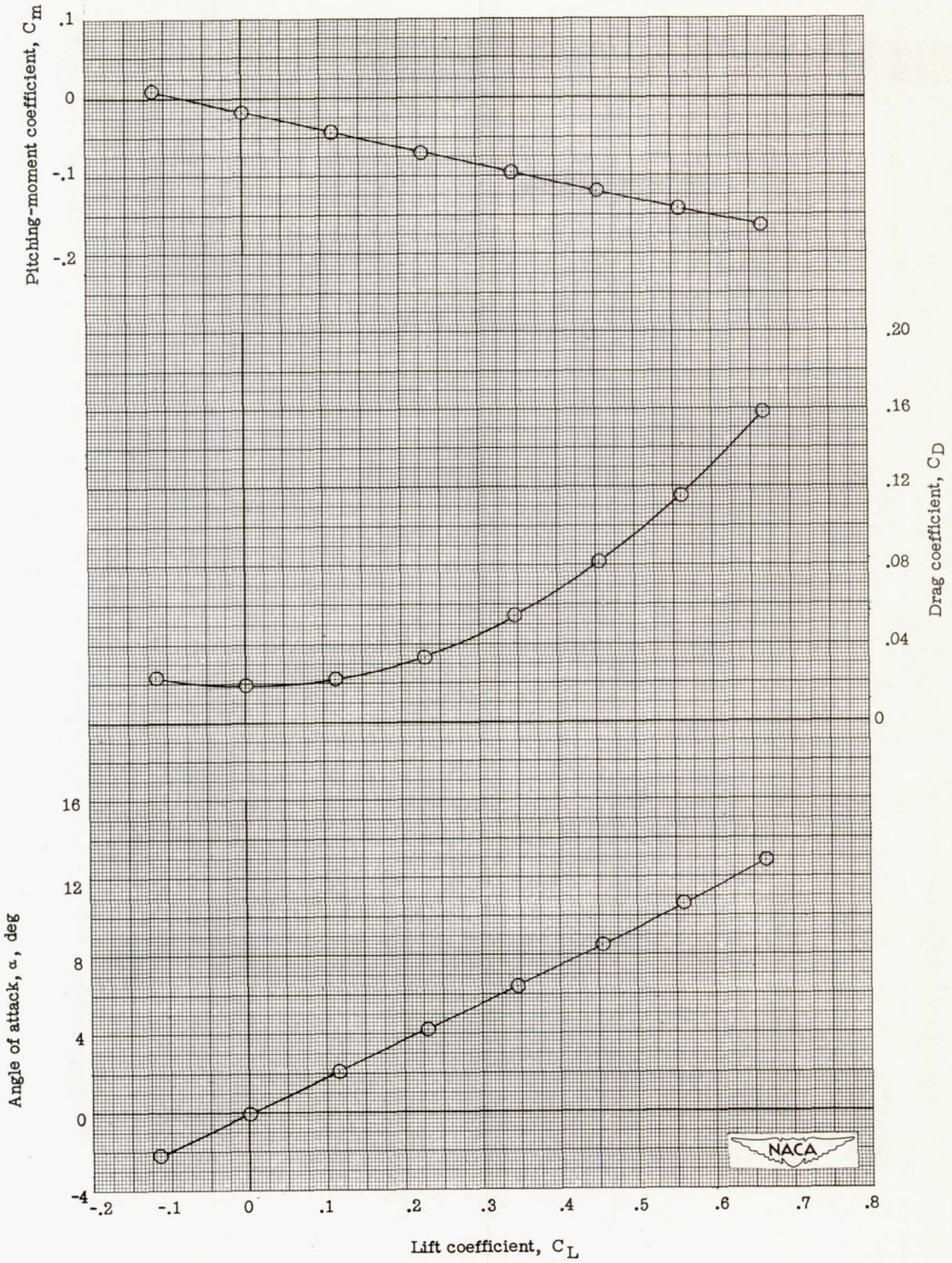


Figure 5.- Aerodynamic characteristics in pitch of body of revolution, based on body frontal area and length. Boundary-layer turbulent.



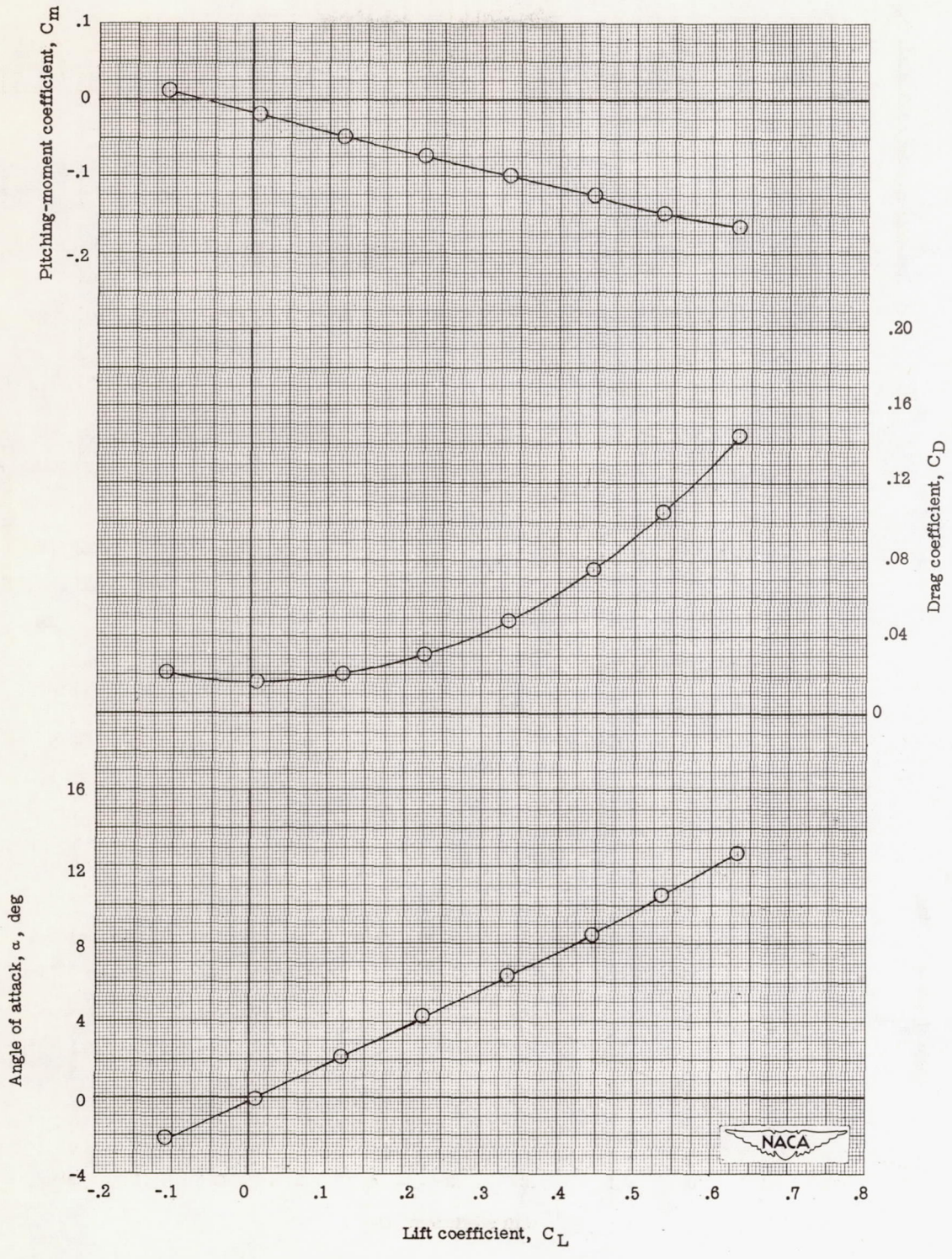
(a) $\Lambda = 10.8^{\circ}$; $\frac{t}{c} = 0.04$.

Figure 6.- Aerodynamic characteristics in pitch of the various wing-body configurations.



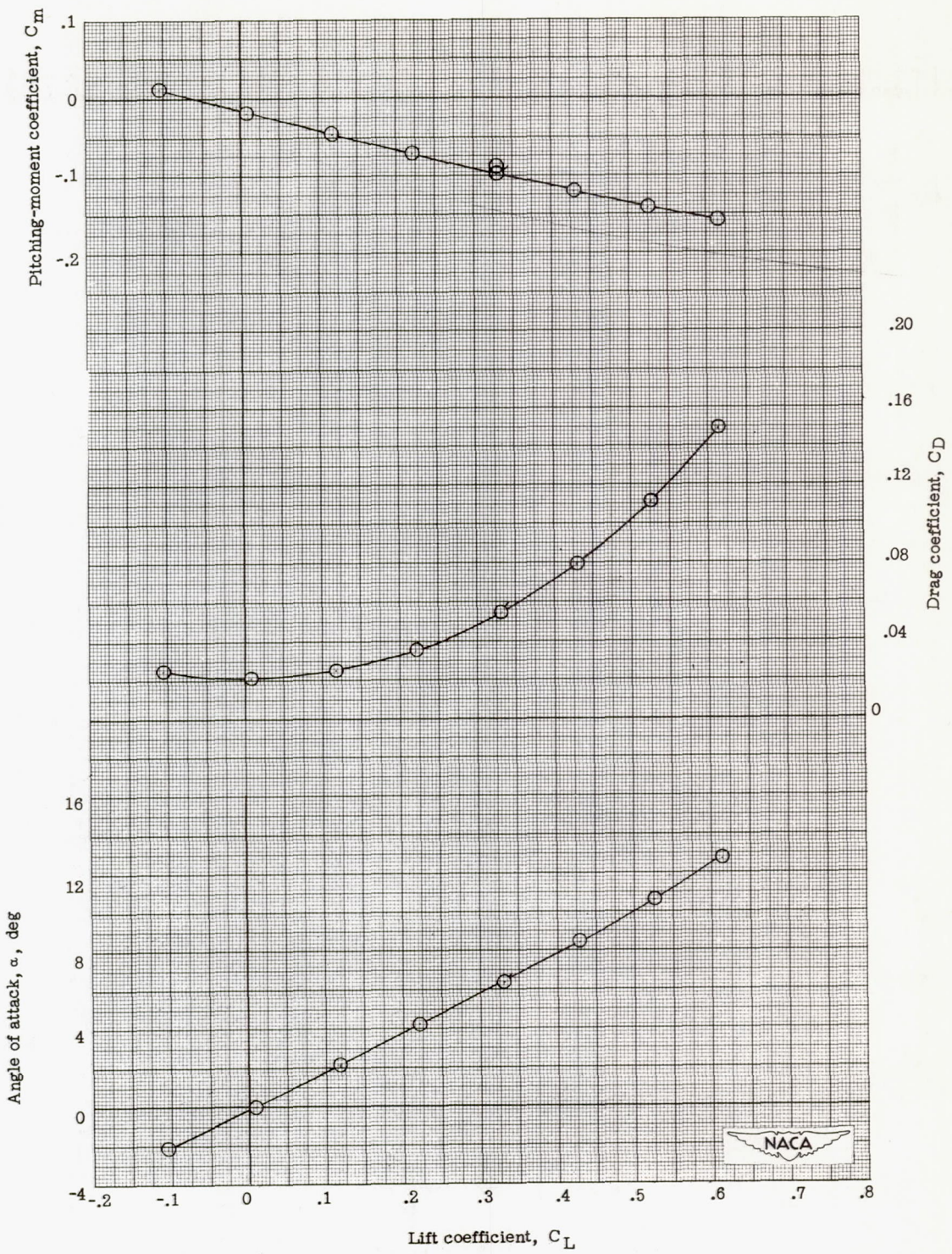
(b) $\Lambda = 35^{\circ}$; $\frac{t}{c} = 0.04$.

Figure 6.- Continued.



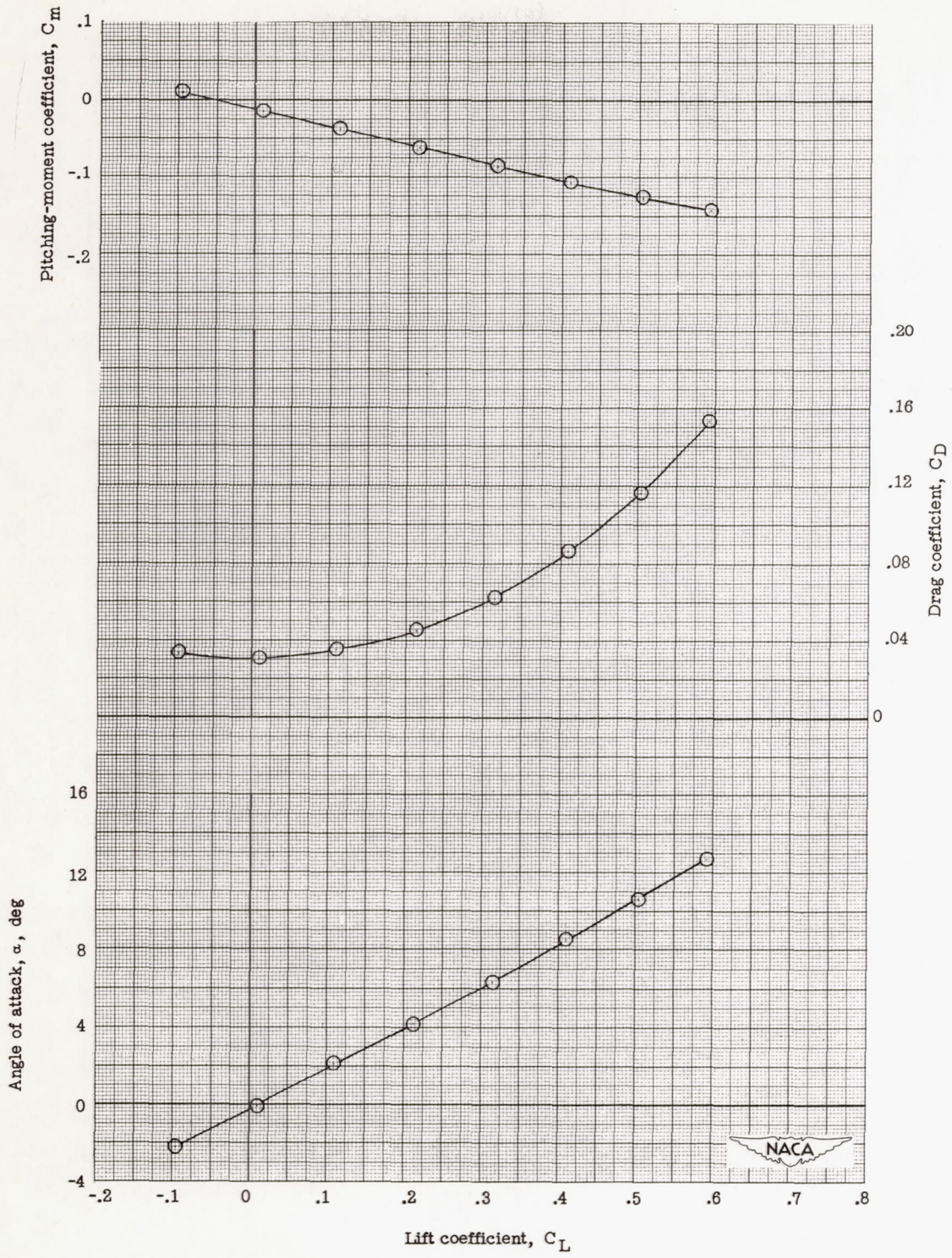
(c) $\Lambda = 47^\circ$; t = 0.04.

Figure 6.- Continued.



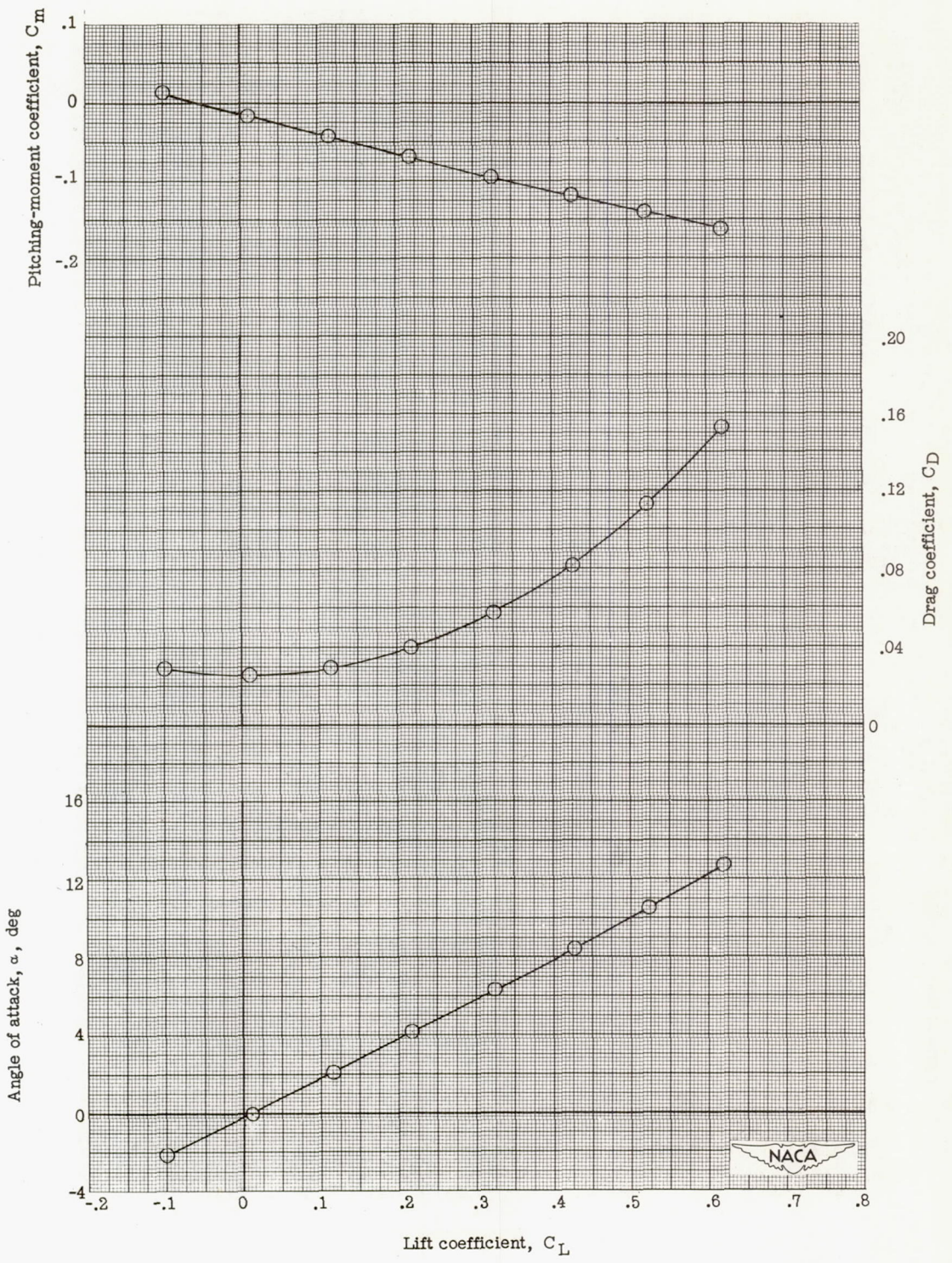
(d) $\Lambda = 47^{\circ}$; t = 0.06.

Figure 6.- Continued.



(e) $\Lambda = 47^\circ$; $\frac{t}{c} = 0.09$.

Figure 6.- Continued.



(f) $\Lambda = 47^\circ$; $\frac{t}{c} = 0.12, 0.06, 0.06$.

Figure 6.- Concluded.

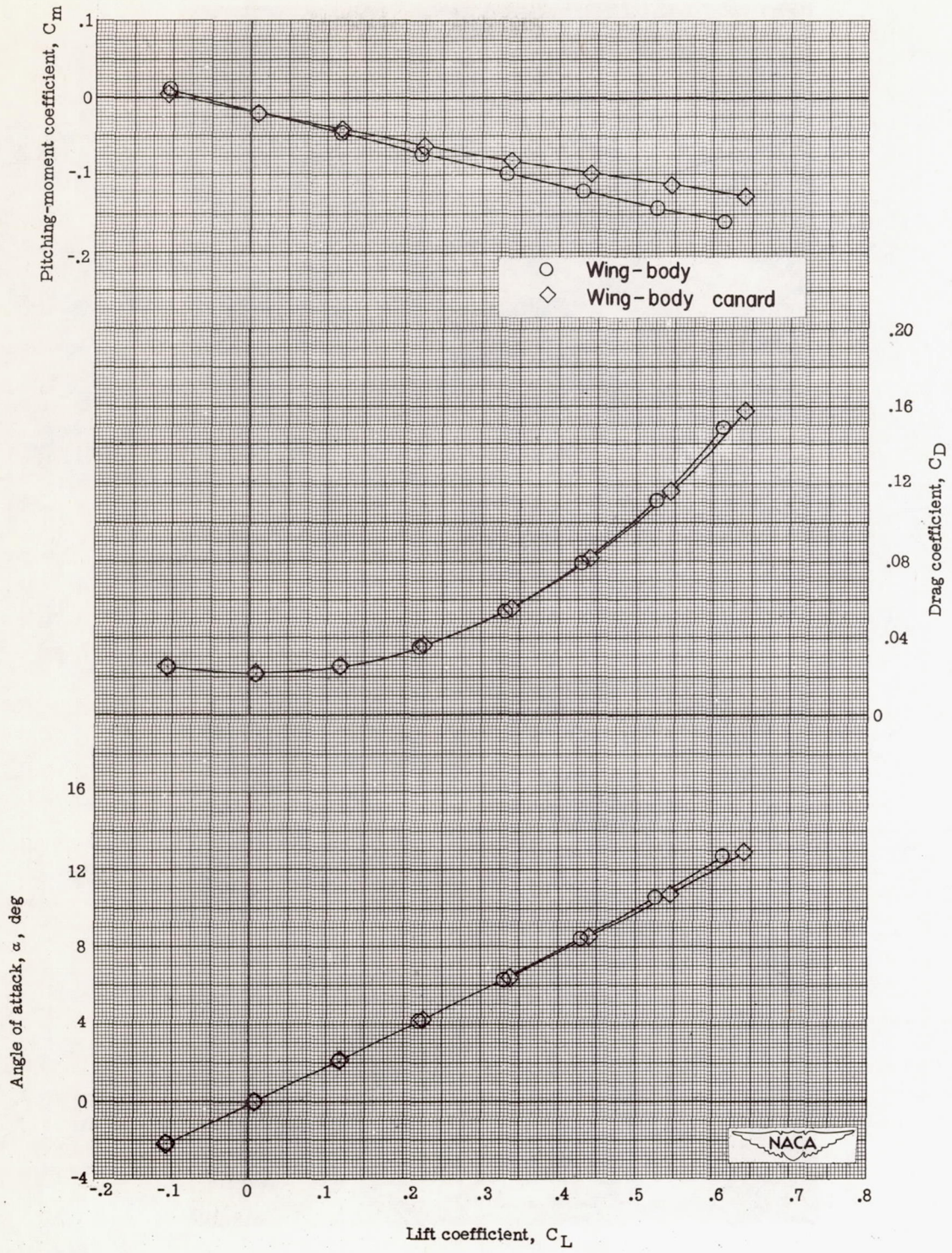
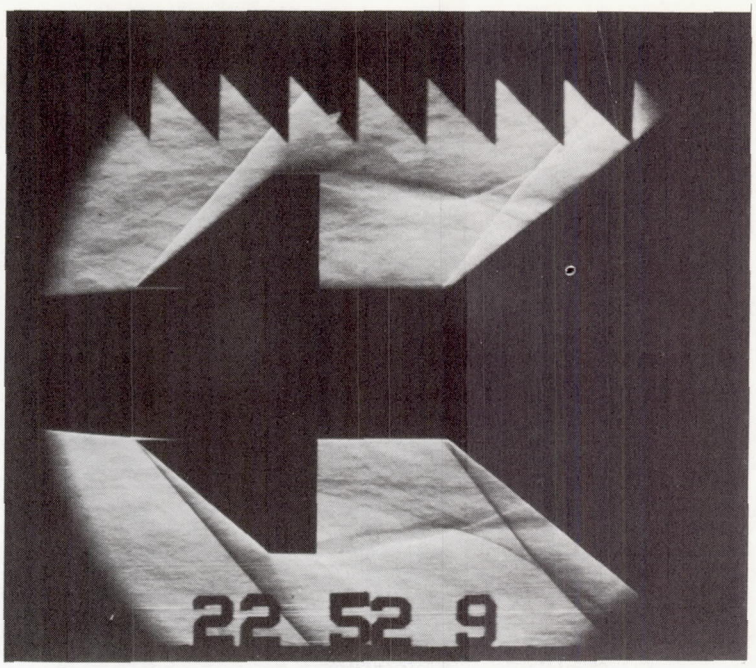
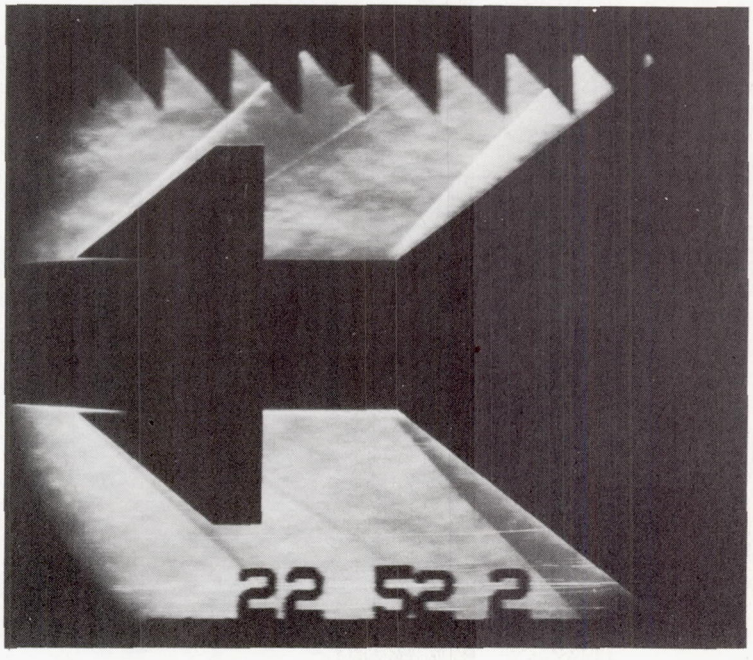


Figure 7.- Aerodynamic characteristics in pitch of a wing-body configuration with and without canard. $\Lambda = 47^\circ$; $\frac{t}{c} = 0.06$.



(a) $\alpha = 12^{\circ}$.

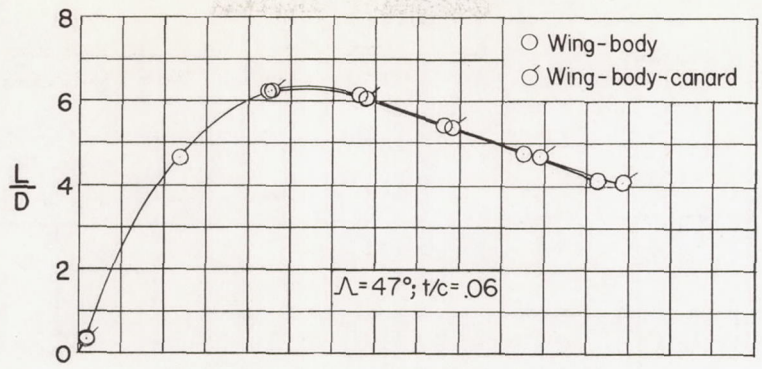


NACA

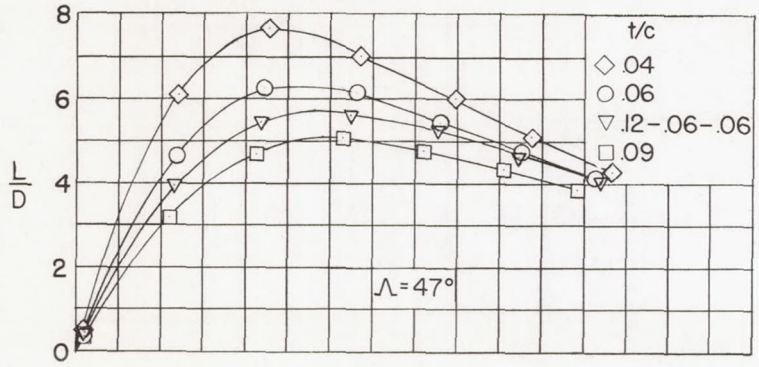
(b) $\alpha = 0^{\circ}$.

L-70848

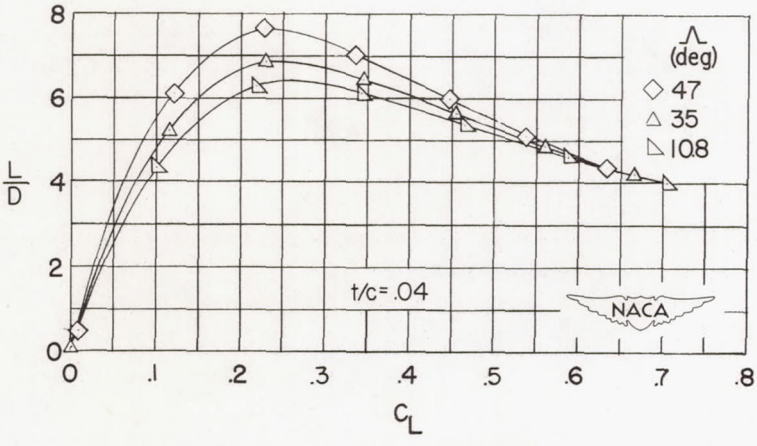
Figure 8.- Schlieren pictures of wing-body canard configuration. $\Lambda = 47^{\circ}$; $\frac{t}{c} = 0.06$.



(a) Effects of canard.



(b) Effects of thickness.



(c) Effects of sweep.

Figure 9.- Variation of lift-drag ratios with lift coefficient for the various wing-body configurations.

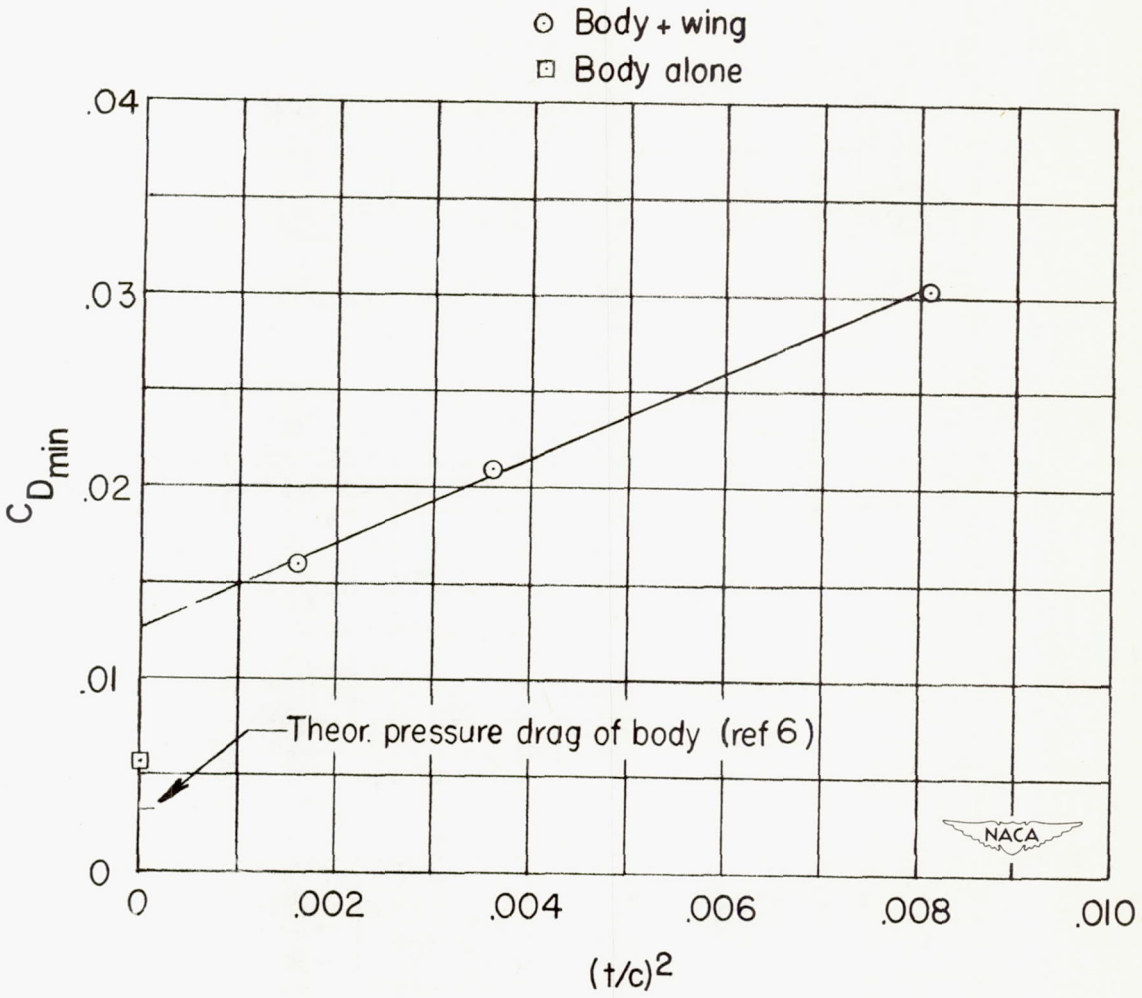


Figure 10.- Variation of minimum drag coefficient with the square of the thickness ratio. $\Lambda = 47^{\circ}$.

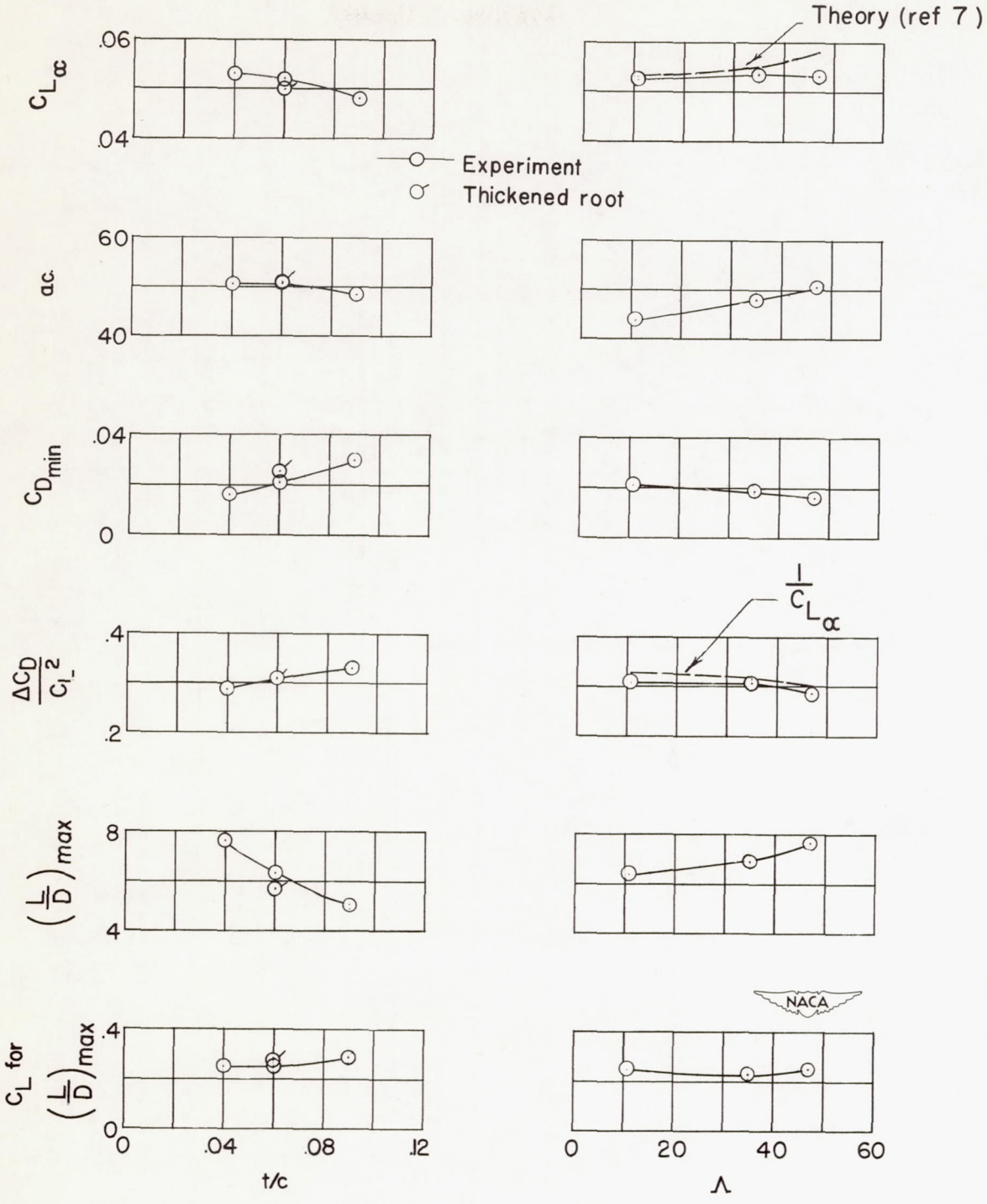


Figure 11.- Summary of the aerodynamic characteristics in pitch of the various wing-body configurations.